JCB Article

Functional interaction between BLM helicase and 53BP1 in a Chk1-mediated pathway during S-phase arrest

Sagar Sengupta,[1] Ana I. Robles,[1] Steven P. Linke,[1] Natasha I. Sinogeeva,[1] Ran Zhang,[1] Remy Pedeux,[1] Irene M. Ward,[3] Arkady Celeste,[2] André Nussenzweig,[2] Junjie Chen,[3] Thanos D. Halazonetis,[4] and Curtis C. Harris[1]

[1]Laboratory of Human Carcinogenesis, [2]Experimental Immunology Branch, National Cancer Institute, National Institutes of Health, Bethesda, MD 20892
[3]Division of Oncology Research, Mayo Clinic, Rochester, MN 55905
[4]Department of Molecular Genetics, The Wistar Institute, Philadelphia, PA 19104

Bloom's syndrome is a rare autosomal recessive genetic disorder characterized by chromosomal aberrations, genetic instability, and cancer predisposition, all of which may be the result of abnormal signal transduction during DNA damage recognition. Here, we show that BLM is an intermediate responder to stalled DNA replication forks. BLM colocalized and physically interacted with the DNA damage response proteins 53BP1 and H2AX. Although BLM facilitated physical interaction between p53 and 53BP1, 53BP1 was required for efficient accumulation of both BLM and p53 at the sites of stalled replication. The accumulation of BLM/53BP1 foci and the physical interaction between them was independent of γ-H2AX. The active Chk1 kinase was essential for both the accurate focal colocalization of 53BP1 with BLM and the consequent stabilization of BLM. Once the ATR/Chk1- and 53BP1-mediated signal from replicational stress is received, BLM functions in multiple downstream repair processes, thereby fulfilling its role as a caretaker tumor suppressor.

Introduction

53BP1, first identified as a p53-interacting protein in a two-hybrid screen (Iwabuchi et al., 1994), is a BRCT motif–containing protein that responds rapidly to different types of DNA damage (Schultz et al., 2000). It is a key transducer protein that is involved in p53 accumulation, as well as G2-M and intra–S-phase checkpoint arrest in response to ionizing radiation (IR; Fernandez-Capetillo et al., 2002; Wang et al., 2002). 53BP1 accumulation at sites of IR-induced double-strand breaks (DSBs) requires γ-H2AX and a physical association between the two proteins (Celeste et al., 2002; Fernandez-Capetillo et al., 2002; Ward et al., 2003a). This response involves the ATM-dependent checkpoint pathway, thought to be constitutively active in certain human cancers (Rappold et al., 2001; DiTullio et al., 2002). 53BP1 and other DNA damage sensor proteins, like NFBD1/MDC1-NBS1, function in parallel interacting pathways and also activate ATM in response to IR (Mochan et al., 2003). The roles of 53BP1 in the DNA damage response and in maintaining genomic stability were confirmed recently in knockout (KO) mice (Ward et al., 2003b).

Though the involvement of H2AX and 53BP1 in response to IR has been extensively investigated, much less is known about the role of sensor proteins during replicational stress. Replicational stress can arise when DNA replication is blocked by DNA damage, induced by agents such as UV radiation or hydroxyurea (HU). The *Saccharomyces cerevisiae* PI3K-related kinase Mec1 and its most closely related mammalian homologue, ATR, are thought to control the cellular responses to replicational stress. ATR carries out its function

The online version of this article includes supplemental material.

Address correspondence to Curtis C. Harris, Chief, Laboratory of Human Carcinogenesis, National Cancer Institute, National Institutes of Health, 37 Convent Dr., Bldg. 37, Rm. 3068, Bethesda, MD 20892-4255. Tel.: (301) 496-2048. Fax: (301) 496-0497. email: Curtis_Harris@nih.gov

Key words: replication arrest; γ-H2AX; p53; homologous recombination; signal transduction

Abbreviations used in this paper: AS, antisense; BS, Bloom's syndrome; DSB, double-strand break; HR, homologous recombination; HU, hydroxyurea; IR, ionizing radiation; KD, kinase defective; KO, knockout; MEF, murine embryo fibroblast; NCS, neocarzinostatin; NHEJ, non-homologous end joining; NHF, normal human fibroblast; SCE, sister chromatid exchange; WT, wild-type.

Supplemental material can be found at:
http://doi.org/10.1083/jcb.200405128

mainly by activating Chk1 through phosphorylation of serines 317 and 345 (Abraham, 2001; Bartek and Lukas, 2003).

BLM, a member of the RecQ family of DNA helicases, has been characterized as a "genome caretaker" (Hickson, 2003). BLM is mutated in Bloom's syndrome (BS) patients, whose cells have abnormal DNA replication and elevated rates of homologous recombination (HR). This is manifested by an accumulation of abnormal replication intermediates and high rates of sister chromatid exchanges (SCEs; van Brabant et al., 2000; Hickson, 2003). BLM can catalyze branch migration of Holliday junctions in vitro, which may prevent the collapse of replication forks and resultant DSBs (Karow et al., 2000). BLM helicase and topoisomerase IIIα cooperate to resolve recombination intermediates during HR (Wu and Hickson, 2003). Thus, BLM has been proposed to function at the interface of replication and recombination and to facilitate the repair of DNA damage.

BLM interacts physically and functionally with a variety of proteins involved in tumor suppression, DNA recombination, and replication. BLM is a responder to DNA damage; rapidly colocalizes to DSBs, as visualized by its colocalization with γ-H2AX (Davalos and Campisi, 2003); binds to p53 (Wang et al., 2001); and transports it to stalled DNA replication forks, resulting in modulation of HR by complementary pathways (Sengupta et al., 2003). Exposure of cells to either IR or replicational stress causes BLM to colocalize and physically interact with RAD51 and RAD54 at stalled DNA replication forks (Wu et al., 2001; Sengupta et al., 2003). The helicase is also part of a putative multiprotein complex (BASC) present at stalled replication foci and colocalizes with BRCA1, MLH1, MRE11-RAD50-NBS1 complex, RPA, ATR, and ATM (Wang et al., 2000). BLM is phosphorylated by ATM kinase following IR, though the ATM-targeted phosphorylation sites are not critical for BLM function in SCE suppression (Beamish et al., 2002). Recently, it has been reported that the NH_2-terminal phosphorylation of Thr-99 and Thr-122 on BLM by ATR is required to recover from S-phase arrest (Davies et al., 2004).

Because BLM, 53BP1, and p53 have the potential to be functionally involved during replicational stress, we sought to investigate their interaction in the context of other major proteins involved in the signal transduction process. Using hTERT immortalized (nontransformed) normal human fibroblasts (NHFs), we demonstrated that endogenous BLM and 53BP1 colocalized rapidly at stalled DNA replication forks and physically interacted with each other. Using isogenic cell lines, gene KO models, and siRNA or antisense (AS)-treated cells, we have shown that BLM facilitated the interaction between p53 and 53BP1 during replicational stress. 53BP1 regulated the accumulation of BLM at sites of DNA damage even in the absence of γ-H2AX. The upstream signal to BLM was predominantly carried through the ATR–Chk1 kinase pathway. Active Chk1 kinase was essential for the accurate focal colocalization of both 53BP1 and BLM at stalled DNA replication forks and the stabilization of the helicase. These results demonstrate that BLM is a responder to DNA damage during replicational stress and imply that functional interactions among BLM, 53BP1, and p53 are required for transmitting the DNA damage signal to downstream repair mechanisms.

Results

BLM is an intermediate responder to replicational stress

In asynchronous NHFs, few nuclear foci of BLM (4–15 per cell) or p53 (2–8 per cell) were present, nor was there significant colocalization of BLM and p53 (unpublished data). These data were similar to findings we have reported previously (Sengupta et al., 2003). As reported elsewhere (Schultz et al., 2000; Rogakou et al., 1999; Anderson et al., 2001), neither γ-H2AX nor 53BP1 foci were visible in nonstressed asynchronous NHFs (unpublished data).

To study replicational stress, cells were synchronized in G0 by growth to confluence, released by replating at low density for 24 h, and then treated with HU for 6 h. Using this protocol, we observed ~60–70% of the cells were present in S-phase (after 6 h of HU treatment), established either by flow cytometry (not depicted) or by BrdU incorporation (Fig. S1 A, available at http://www.jcb.org/cgi/content/full/jcb.200405128/DC1). We and others have demonstrated that, during HU treatment, BLM accumulates at stalled DNA replication forks, as visualized by pulse-labeled BrdU incorporation (Sengupta et al., 2003) or PCNA staining (Davies et al., 2004). To determine whether γ-H2AX was also involved in the response to HU-induced stalled DNA replication forks, we performed a time course for the accumulation of endogenous γ-H2AX protein and foci, as well as the colocalization of γ-H2AX foci with pulse-labeled BrdU (after DNase treatment). The nuclei were visualized after preextraction, which removed the soluble nucleoplasm. Hence, only the proteins that were bound to the insoluble matrix were visualized. During HU treatment, γ-H2AX protein increased with time (Fig. 1 C, a). Correspondingly, γ-H2AX foci accumulated and colocalized appreciably with BrdU within 30 min as previously reported (Fig. 1 A; Davalos and Campisi, 2003). Although endogenous 53BP1 protein levels remained unchanged during HU treatment (Fig. 1 C, b), 53BP1 foci appeared with similar kinetics as γ-H2AX foci (Fig. 1 A). BLM and p53 protein levels increased with similar kinetics (Fig. 1 C, c and d). BLM foci were detected within 30 min and increased in number and degree of colocalization (as measured by colocalization factor, defined in Materials and methods) with BrdU (Sengupta et al., 2003; unpublished data). Moreover, a time-dependent enhancement of BLM and 53BP1 foci colocalization was also observed (Fig. 1, A and B). BLM foci appeared earlier than p53 foci, and the number of p53 foci was always less than the number of γ-H2AX, 53BP1, or BLM foci. Within 6 h, almost all BLM and p53 foci colocalized with 53BP1 foci (Fig. 1, A and B). The colocalization factors for the same pairs of foci were much less when the cells were subjected to the same synchronization protocol, but were not treated with HU, indicating that the colocalization were a result of HU-mediated replicational stress and not due to the synchronization protocol (Fig. S1 B). These results indicate that γ-H2AX, 53BP1, BLM, and p53 likely function in the same response pathway.

We next investigated the rate of focal accumulation and colocalization of proteins involved in different DNA repair pathways like HR, in which proteins like MRE11 and RAD51 are involved. The colocalization of MRE11 and RAD51 foci with sites of stalled DNA replication forks (as measured by their colocalization with 53BP1 foci) never ex-

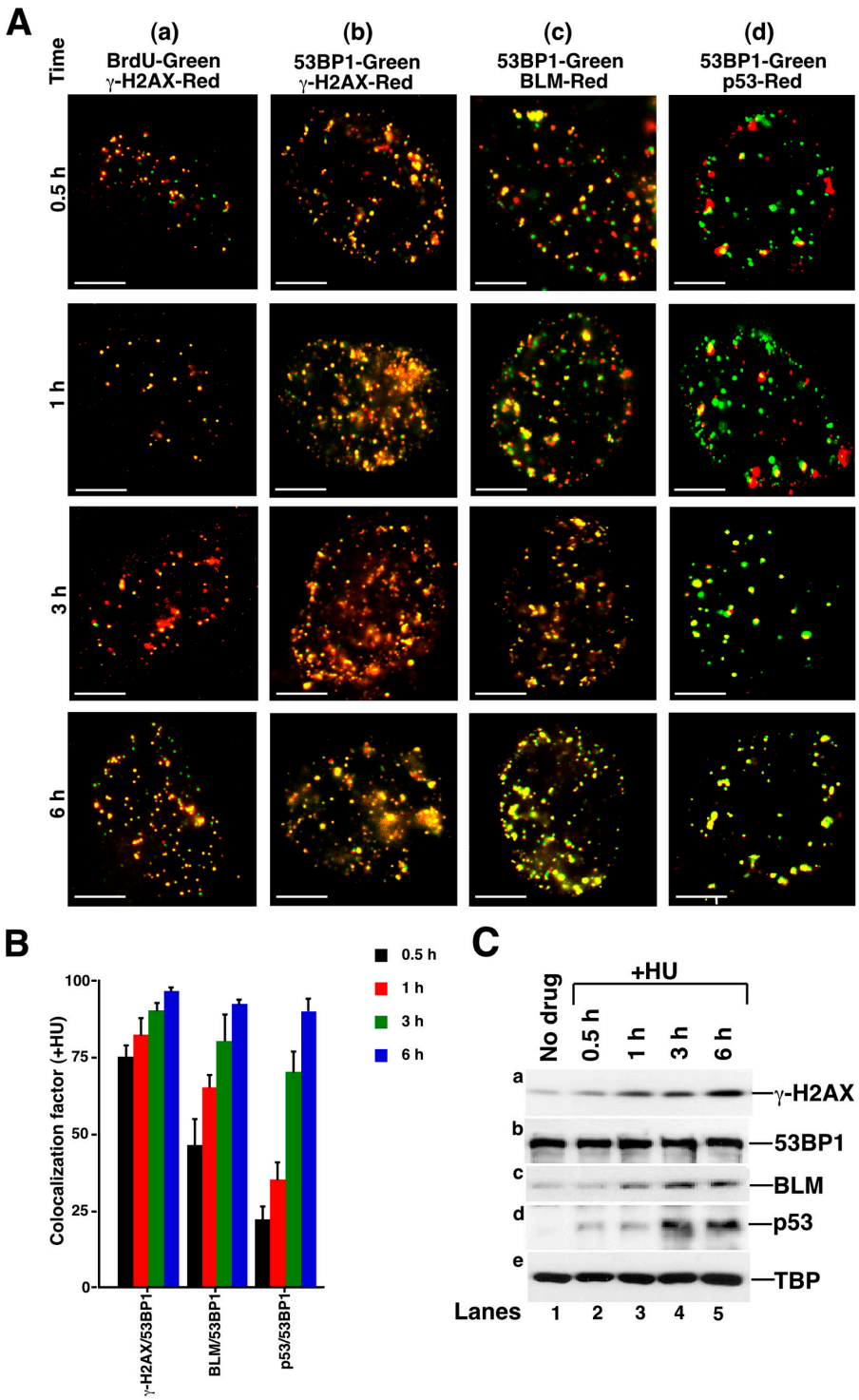

Figure 1. **γ-H2AX, 53BP1, BLM, and p53 colocalize and accumulate with similar kinetics.** (A) Time course of the accumulation of BrdU, γ-H2AX, 53BP1, BLM, and p53 foci after HU treatment. NHFs were contact inhibited, split at low dilution, and treated with HU for the indicated time intervals. BrdU staining was done on washed cells and incubated with the nucleotide analogue for 10 min. Immunofluorescence was performed with antibodies against BrdU/γ-H2AX (a); 53BP1 (monoclonal)/γ-H2AX (b); 53BP1 (monoclonal)/BLM (ab476) (c); and 53BP1 (monoclonal)/p53 (CM1) (d). Bars, 5 μm. (B) Quantitation of A. The graphs represent mean ± SD. (C) The accumulation of proteins after HU treatment. Western blots were performed with anti-γ-H2AX (a), anti-53BP1 (polyclonal; b), anti-BLM (C-18) (c), anti-p53 (DO-1) (d), and anti-TBP antibodies (e).

ceeded 45% even after 6 h of HU treatment (Fig. S1, C and D). Thus, although MRE11 and RAD51 apparently function in the same replicational stress pathway as γ-H2AX, 53BP1, BLM, and p53, they also appear to possess distinct divergent localization and functions.

BLM and 53BP1 have an inter-regulatory relationship

We have previously demonstrated that BLM, p53, and RAD51 colocalize and physically interact as part of a multiprotein complex at the sites of stalled DNA replicational forks. Moreover, BLM is involved in the recruitment of p53 to these sites (Sengupta et al., 2003). As an extension of our previous work, we found that 53BP1 and p53 were also present in BLM immunoprecipitates of HU-treated NHFs (Fig. 2 A). Reciprocally, 53BP1 was also present in p53 immunoprecipitates (Fig. 2 B). Due to possible steric interference, BLM could not be detected in p53 immunoprecipitates (Wang et al., 2001; unpublished data). BLM immunoprecipitates from p53-deficient NHF E6 cells contained 53BP1 (Fig. 2 C). Consistent with this finding, BLM

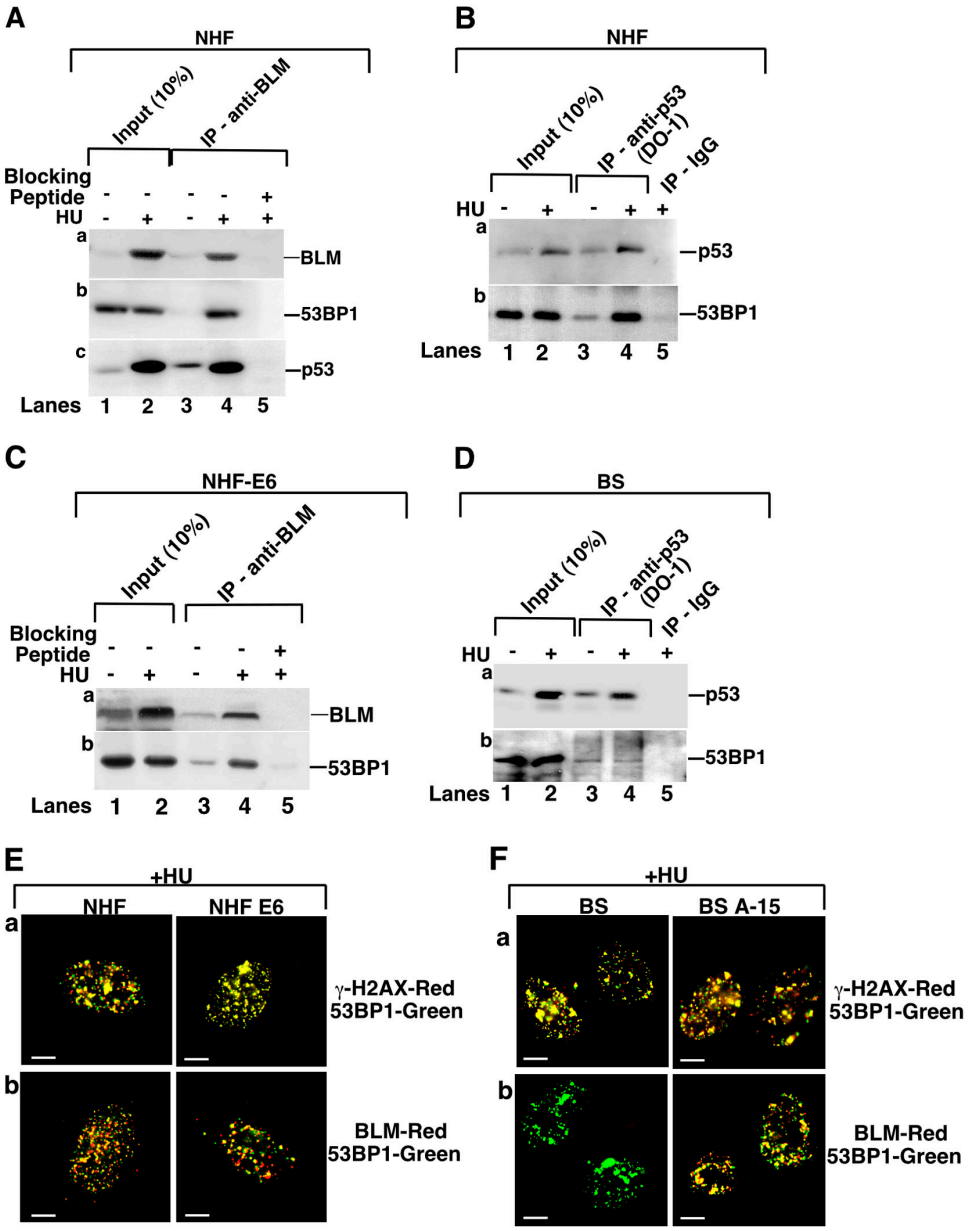

Figure 2. **53BP1 interacts with p53 via BLM.** (A and C) The immunoprecipitation of BLM revealed 53BP1 in NHFs and NHF E6. NHFs (A) and NHF E6 (C) were either left asynchronous (lane 1) or contact inhibited, split at low dilution, and treated with HU (lane 2) for 6 h. 400 μg of lysates were immunoprecipitated with antibodies against BLM (C-18) in the absence (lanes 3 and 4) or presence (lane 5) of the blocking peptide. Input (lanes 1 and 2) indicates 10% of the lysate was used for immunoprecipitation. The efficiency of immunoprecipitation was verified with self-antibody (a). The BLM immunoprecipitates were probed with anti-53BP1 (polyclonal; for both A and C, b) and anti-p53 (DO-1) (for A only, c) antibodies. Lanes 1 and 3, minus HU; lanes 2, 4, and 5, plus HU. (B and D) Immunoprecipitation of p53 revealed 53BP1 in NHFs, but not in BS. Same as in A and C, except NHFs were used in B and BS in D. Immunoprecipitation was done with antibodies against p53 (DO-1) (lanes 3 and 4) or against the corresponding IgG (lane 5). The p53 immunoprecipitates were probed with polyclonal anti-53BP1 antibody (b). (E) γ-H2AX, 53BP1, and BLM colocalize in the absence of p53. NHFs or NHF E6 were prepared as in A and treated with HU for 6 h. Immunofluorescence was performed with antibodies against γ-H2AX/53BP1 (monoclonal; a) and BLM (ab476)/53BP1 (monoclonal; b). Bars, 5 μm. (F) 53BP1 accumulates at the sites of stalled replication forks even in the absence of BLM. Same as in E except, BS and BS A-15 cells were used. Bars, 5 μm.

and 53BP1 accumulates at stalled replication forks in HU-arrested cells, and 53BP1 colocalized with both γ-H2AX and BLM foci in p53-deficient cells (Fig. 2 E), indicating that p53 is dispensable for focal accumulation and physical interaction of BLM and 53BP1. Though p53 immunoprecipitates from BLM-deficient BS cells contained low levels of 53BP1, the p53–53BP1 interaction was not enhanced by replicational stress (Fig. 2 D). Thus, BLM facilitated the physical interaction between 53BP1 and p53 in vivo. Interestingly, 53BP1 accumulated at γ-H2AX foci in synchronized HU-arrested cells even in the absence of BLM protein (Fig. 2 F, b), suggesting that BLM was dispensable for 53BP1 focal accumulation.

To investigate if 53BP1 affected the localization of BLM or p53, experiments were performed using murine or human cells, where 53BP1 was either absent or decreased (Fig.

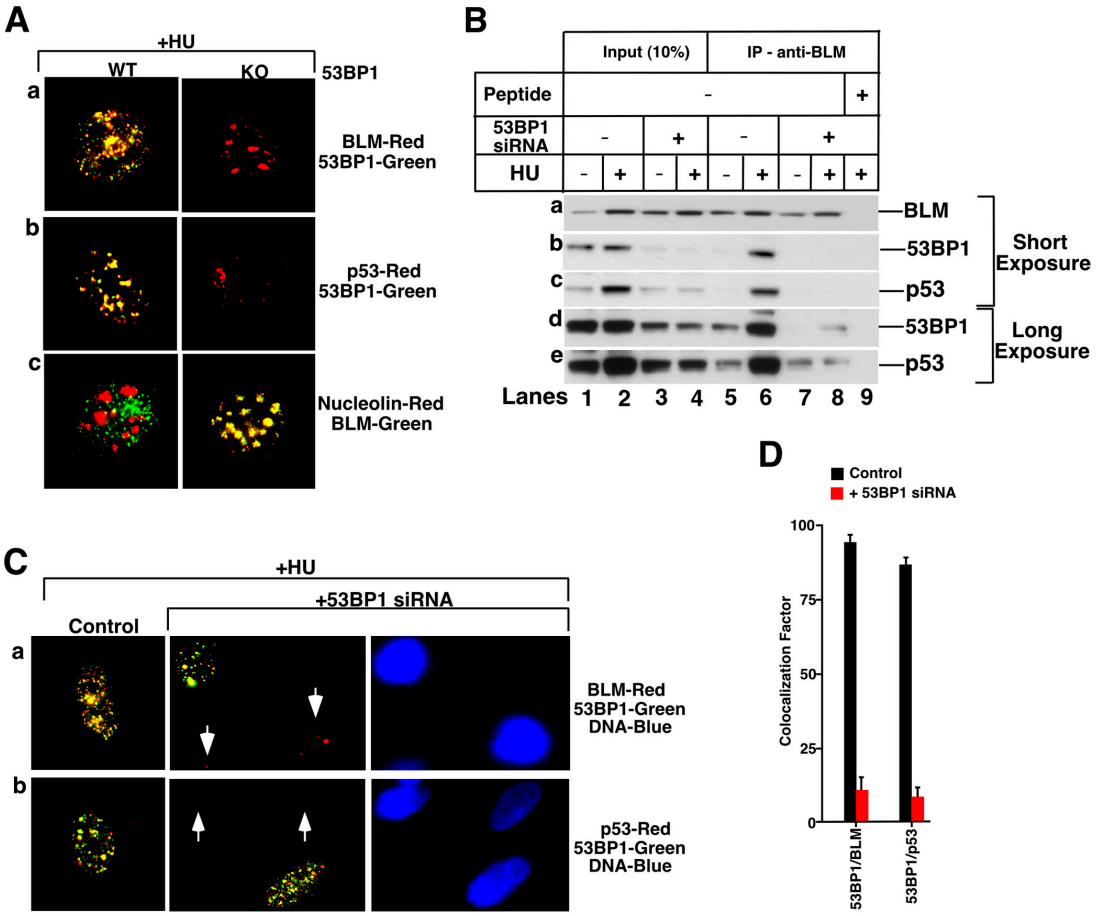

Figure 3. **53BP1 regulates the accumulation of BLM.** (A) Absence of 53BP1 leads to nucleolar accumulation of BLM in KO MEFs. WT or 53BP1 KO MEFs were treated with HU for 6 h. Immunofluorescence was performed with antibodies against BLM (ab476)/53BP1 (monoclonal; a); p53 (CM1)/53BP1 (monoclonal; b); and BLM (ab476)/nucleolin (c). (B) The interaction of BLM with 53BP1 and p53 is decreased in 53BP1siRNA-treated cells. Control (lanes 1 and 2) or 53BP1 siRNA-transfected (lanes 3 and 4) NHFs were contact inhibited, split at low dilution, and grown either in the absence (lanes 1 and 3) or presence (lanes 2 and 4) of HU for 6 h. 400 μg of lysates were immunoprecipitated with antibodies against BLM (C-18) (lanes 5–9) in the absence (lanes 5–8) or presence (lane 9) of the blocking peptide. Input (lanes 1–4) indicates 10% of the lysate was used for immunoprecipitation. The efficiency of immunoprecipitation was verified with BLM (ab476) antibody (a). Antibodies used for the detection of other proteins in BLM immunoprecipitation were anti-53BP1 (polyclonal; b and d) and anti-p53 (DO-1) (c and e). Lanes 1, 3, 5, and 7, minus HU; lanes 2, 4, 6, 8, and 9, plus HU. Panels d and e are longer exposures of the same blots in b and c. (C) The lack of 53BP1 prevents the accumulation of BLM and p53. Transfection and treatment were done as in B. Immunofluorescence was performed with antibodies against BLM (ab476)/53BP1 (monoclonal)/DNA (DAPI) (a) and p53 (CM1)/53BP1 (monoclonal)/DNA (DAPI) (b). Fields were chosen that contained a cell in which 53BP1 expression was not suppressed as an internal control for cells lacking expression of 53BP1. Arrows indicate the position of cells lacking 53BP1 expression. (D) Quantitation of C. The histogram represents mean ± SD.

3). The primary murine embryo fibroblasts (MEFs) used at passage 2–3 retained their wild-type (WT) p53 gene sequence and functions (induction of p21 due to DNA damage; unpublished data). In WT MEFs, 53BP1 colocalized with both BLM and p53 in discrete foci outside nucleoli during HU treatment. However, in HU-treated 53BP1 KO MEFs, BLM staining was detected in nucleoli, whereas p53 foci were almost completely absent. Nucleolar sequestration of BLM in KO MEFs was confirmed by colocalization of BLM with nucleolin (Fig. 3 A).

The results with murine cells were cross-validated in NHFs, in which 53BP1 was decreased by using a previously published siRNA (DiTullio et al., 2002). The same synchronization and HU treatment protocol was used, except that two sequential 53BP1 siRNA transfections were conducted just before growth to confluence. Both the control and 53BP1 siRNA-transfected cell populations contained ∼60% S-phase cells after 6 h of HU treatment, as analyzed by flow cytometry and BrdU incorporation (Fig. S2, A and B, available at http://www.jcb.org/cgi/content/full/jcb.200405128/DC1; and not depicted). 53BP1 depletion was not complete, which led to the appearance of residual protein and 53BP1 foci in ∼30% of the HU-treated cells (Fig. 3, B and C). In control siRNA-transfected cells (and also a subpopulation of 53BP1 siRNA-treated cells), 53BP1 colocalized extensively with BLM and p53 (Fig. 3, C and D), whereas BrdU staining colocalized with BLM and 53BP1 (Fig. S2 C, a and b). Although 53BP1 siRNA-treated cells exhibited stalled replication forks as visualized by BrdU staining, the focal accumulation of both BLM and p53 foci was greatly diminished when compared with control cells after HU treatment (Fig. 3, C and D; and Fig. S2 C, c). BLM accumula-

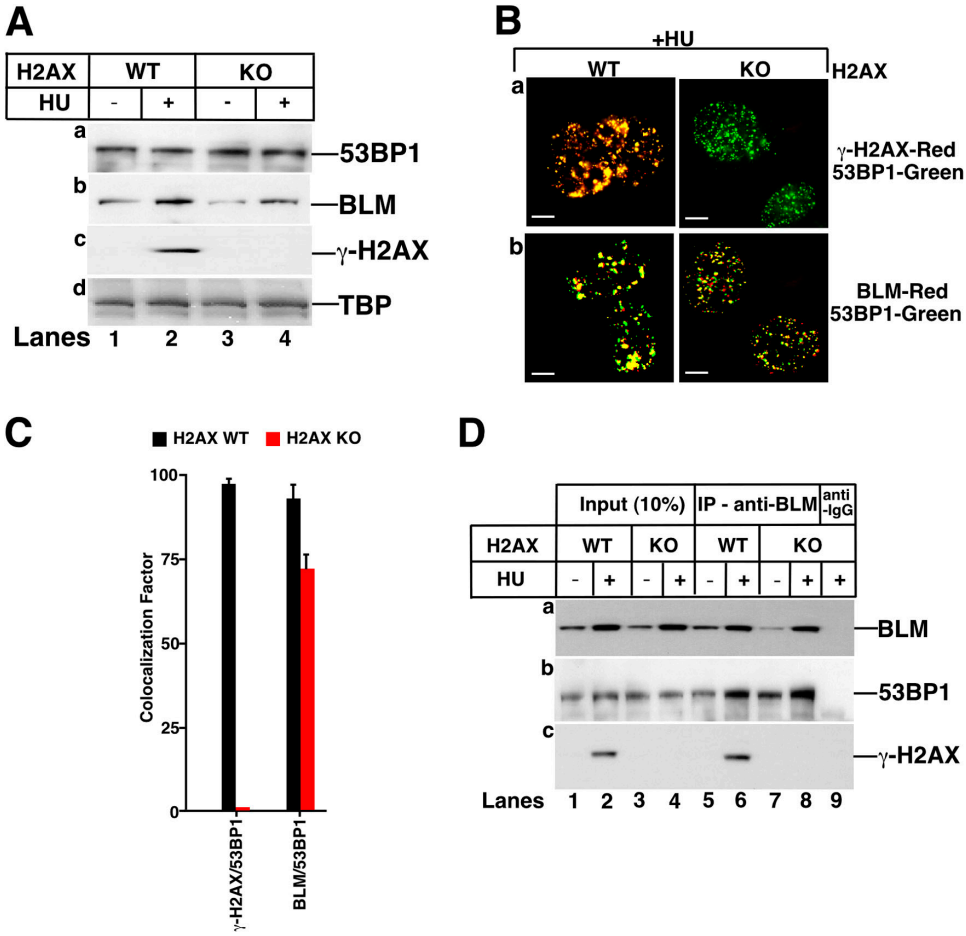

Figure 4. **53BP1 and BLM can accumulate and physically interact independently of γ-H2AX.** (A) The accumulation of proteins in WT and H2AX KO MEFs after HU. H2AX WT (lanes 1 and 2) and KO (lanes 3 and 4) cells were contact inhibited, split at low dilution, and grown either in the absence (lanes 1 and 3) or presence (lanes 2 and 4) of HU for 6 h. Western blots were performed with anti-53BP1 (polyclonal; a), anti-BLM (ab476) (b), anti-γ-H2AX (c), and anti-TBP antibodies (d). (B) 53BP1 and BLM accumulate at the sites of stalled replication forks even in the absence of γ-H2AX. MEFs were treated as in A. Immunofluorescence was performed with antibodies against γ-H2AX /53BP1 (monoclonal; a) and BLM (ab476)/53BP1 (monoclonal; b). Bars, 5 μm. (C) Quantitation of B. The histogram represent mean ± SD. (D) BLM interacts with 53BP1 and BLM even in the absence of H2AX. WT (lanes 1 and 2) or H2AX KO (lanes 3 and 4) MEFs were prepared as in A and were either left untreated (lanes 1 and 3) or treated with HU (lane 2 and 4) for 6 h. 400 μg of lysates were immunoprecipitated with antibodies against BLM (ab476) (lanes 5–8) or corresponding IgG (lane 9). Input (lanes 1–4) indicates 10% of the lysate used for immunoprecipitation. The efficiency of immunoprecipitation was verified with BLM (ab476) antibody (a). Antibodies used for the detection of other proteins in BLM immunoprecipitation were anti-53BP1 (polyclonal) (b) and γ-H2AX (c). Lanes 1, 3, 5, 7, minus HU; lanes 2, 4, 6, 8, and 9, plus HU.

tion in the nucleoli of 53BP1-depleted NHFs was much less than in the 53BP1 KO MEFs, which probably reflects a species difference, as has been reported for WRN, another member of the RecQ family of helicases (Suzuki et al. 2001). Thus, lack of 53BP1 prevents the accumulation of BLM and p53 at stalled DNA replication forks in both human and murine cells.

To confirm the interaction of 53BP1 and BLM, immunoprecipitations were performed with BLM antibody in cell lysates from control and 53BP1siRNA-treated NHFs. Equivalent levels of BLM were immunoprecipitated in HU-treated control and 53BP1 siRNA-treated cells. Although BLM formed a complex with 53BP1 and p53 in control cells during replicational stress, the amount of p53 and its complex with BLM was diminished in cells in which 53BP1 levels were decreased (Fig. 3 B, compare lanes 6 and 8). These results indicate that 53BP1 is upstream of BLM and regulates its focal accumulation.

γ-H2AX is dispensable for the focal accumulation of BLM and 53BP1 during replicational stress

Exposure of MEFs to neocarzinostatin (NCS), which also causes DSBs like IR (Povirk et al., 1988), did not change the protein level of 53BP1 (unpublished data). Similar to IR, 53BP1 focal accumulation was diminished in NCS-treated H2AX KO MEFs when compared with WT MEFs (Fig. S2 D). 53BP1 protein levels were similar in WT and KO H2AX MEFs after HU treatment. BLM was induced to similar levels in both genotypes in the presence of HU (Fig. 4 A). However, HU-dependent accumulation of both BLM and 53BP1 foci occurred in both H2AX WT and KO MEFs (Fig. 4 B). The colocalization factor for BLM/53BP1 was close to 75% in KO MEFs (Fig. 4 C). Hence, unlike IR, H2AX was dispensable for the accumulation of 53BP1 and BLM to the replicational forks. Equivalent BLM immunoprecipitates obtained from HU-treated WT and KO H2AX MEFs also contained 53BP1 (Fig. 4 D, compare lanes 6 and

8). These results indicate that BLM and 53BP1 form foci and physically associate during replicational stress even in the absence of γ-H2AX.

Chk1 regulates the accumulation of 53BP1 and BLM foci

Chk1 is involved in IR-induced S and G2/M checkpoints in mammalian cells. Activated pChk1 kinase phosphorylates targets like Cdc25C and p53 (Bartek and Lukas, 2003). To determine whether replicational stress signaling to 53BP1/BLM was transmitted through the ATR and Chk1 kinase pathway, we used two independent approaches: a Chk1 siRNA (Zhao et al., 2002) or a Chk1 AS construct (Shieh et al., 2000). The reduction in Chk1 expression by siRNA (Fig. 5 A) or AS transfection (Fig. 5 D, lane 4) resulted in reduced phosphorylation of Chk1 at Ser-317 (pChk1) during HU treatment.

Using the same synchronization and HU treatment protocol, two sequential Chk1 siRNA transfections were conducted just before growth to confluence. Both the control and Chk1 siRNA-transfected cell populations contained ∼60% S-phase cells after 6 h of HU treatment as analyzed by flow cytometry and BrdU incorporation. However, longer durations of Chk1 siRNA transfection did alter cell cycle profile, hence the shorter time point was chosen (unpublished data). Chk1 depletion was not complete, which led to the appearance of residual protein and pChk1 foci in ∼10% of the HU-treated cells (Fig. 5, A and B; and Fig. S3 A, available at http://www.jcb.org/cgi/content/full/jcb.200405128/DC1). In control cells and in cells where Chk1 was not down-regulated, pChk1 colocalized extensively with BLM and 53BP1. However, the absence of pChk1 foci was associated with a lack of BLM or 53BP1 foci (Fig. 5 B and Fig. S3 A) and decrease in the level of colocalization (Fig. 5 C and Fig. S3 B). The Chk1 siRNA-treated cells still stained with BrdU, indicating the presence of stalled replication forks due to HU treatment (Fig. S3 C, a). Transfection of control siRNA did not cause a depletion of pChk1 foci nor altered its subsequent colocalization with BrdU foci (Fig. S3 C, b).

These results suggested that Chk1 was upstream of 53BP1 and BLM in response to HU. The depletion or overexpression of Chk1 did not alter the protein levels of 53BP1 (Fig. 5, A and D). In contrast, overexpression of Chk1 in the presence of HU resulted in enhanced BLM accumulation, above the level obtained with HU alone (Fig. 5 D, lane 3). Conversely, the abrogation of endogenous Chk1 expression by Chk1 AS or Chk1 siRNA led to decreased BLM accumulation (Fig. 5, A and D). To determine whether or not the kinase activity of Chk1 was essential for BLM accumulation, we used UCN-01, a drug known to inhibit the kinase activity of Chk1, but not that of ATR (Busby et al., 2000). Cotreatment of UCN-01 for a short duration of 6 h did not cause a change in the cell cycle profile of HU-treated NHFs. Longer durations of UCN-01 treatment did alter cell cycle profile, hence the shorter time point was chosen (unpublished data). Because UCN-01 does not affect the upstream signaling pathways to Chk1, resulting in its phosphorylation (Busby et al., 2000), NHFs treated with UCN-01 showed similar levels of either Chk1 or pChk1. The level of BLM (but not 53BP1) decreased after UCN-01 treatment (Fig. 5 D, lane 5). Though pChk1 foci were visible, very little BLM/pChk1 colocalization was observed. Similarly, pChk1 and 53BP1 did not colocalize in UCN-01–cotreated NHFs (Fig. 5 E). Hence, activated Chk1 kinase may be required for the correct colocalization and accumulation of BLM foci at sites of stalled DNA replication forks.

ATR is the direct upstream regulator of Chk1 (Abraham, 2001; Bartek and Lukas, 2003). To confirm the ATR/Chk1/53BP1/BLM/p53 pathway, we first used a pair of isogenic U2OS cells expressing doxycycline-inducible Flag-tagged ATR and ATR-kd (ATR-kinase defective) proteins (Nghiem et al., 2002). Though the formation of ATR, pChk1, BLM, and 53BP1 foci were not affected, a high percentage of colocalization was observed only in WT ATR but not in ATR-kd cells (Fig. S3, B and D). As a second approach, NHFs were cotreated with HU and either caffeine, LY294002, or wortmannin. The drug concentrations were selected so that ATM/ATR (for caffeine) or all known PI3-kinases (for LY294002 and wortmannin) would be inhibited (Sarkaria, 2003). Caffeine, LY294002, or wortmannin treatments diminished the phosphorylation of Chk1 (Fig. 5 F and not depicted). Neither the protein levels of 53BP1 nor the cell cycle profile of HU-treated NHFs were altered by 6-h cotreatment with caffeine, LY294002, or wortmannin (unpublished data). Similar to the effect with Chk1 siRNA, AS Chk1, and UCN-01 (Fig. 5 D), caffeine and LY294002 inhibited BLM accumulation in response to HU treatment (Fig. 5 F). Caffeine, LY294002, and wortmannin also diminished focal colocalization of BLM with pChk1 or 53BP1 after HU treatment (Fig. 5, C and G; and not depicted). These results indicated that BLM was possibly phosphorylated, stabilized, and subsequently colocalized with replicational forks in an ATR- and Chk1-dependent manner.

Chk1-mediated phosphorylation of BLM

To demonstrate Chk1-mediated in vitro phosphorylation, reactions were performed using purified substrates and Chk1 (WT) and kinase defective (KD; Fig. S4 A, available at http://www.jcb.org/cgi/content/full/jcb.200405128/DC1). As reported earlier (Shieh et al., 2000), p53 was phosphorylated by Chk1 WT, but not by Chk1 KD (Fig. 6 A, lanes 1–4). Chk1 WT and not Chk1 KD also phosphorylated BLM in a dose-dependent manner (Fig. 6 A, lanes 5–8).

Recently, it has been reported that the phosphorylation of NH_2-terminal BLM on Thr-99 and Thr-122 is mediated by ATR (Davies et al., 2004). To investigate whether or not Chk1 can phosphorylate these BLM mutants, we performed in vitro phosphorylation reactions. WT Chk1 (but not the KD mutant) can phosphorylate the single (T99A and T122A) and double (T99A/T122A) mutants, and WT BLM to similar extents. The in vitro phosphorylation reactions were done in the context of both the truncated NH_2-terminal (1–212) region of BLM (Fig. S4 B) and the full-length protein (Fig. 6 B).

To determine whether or not endogenous Chk1 interacted with endogenous BLM in vivo during replicational stress, reciprocal immunoprecipitations were performed in NHF cells using either BLM or Chk1 antibody. Chk1 was present in BLM immunoprecipitates, whereas BLM was also

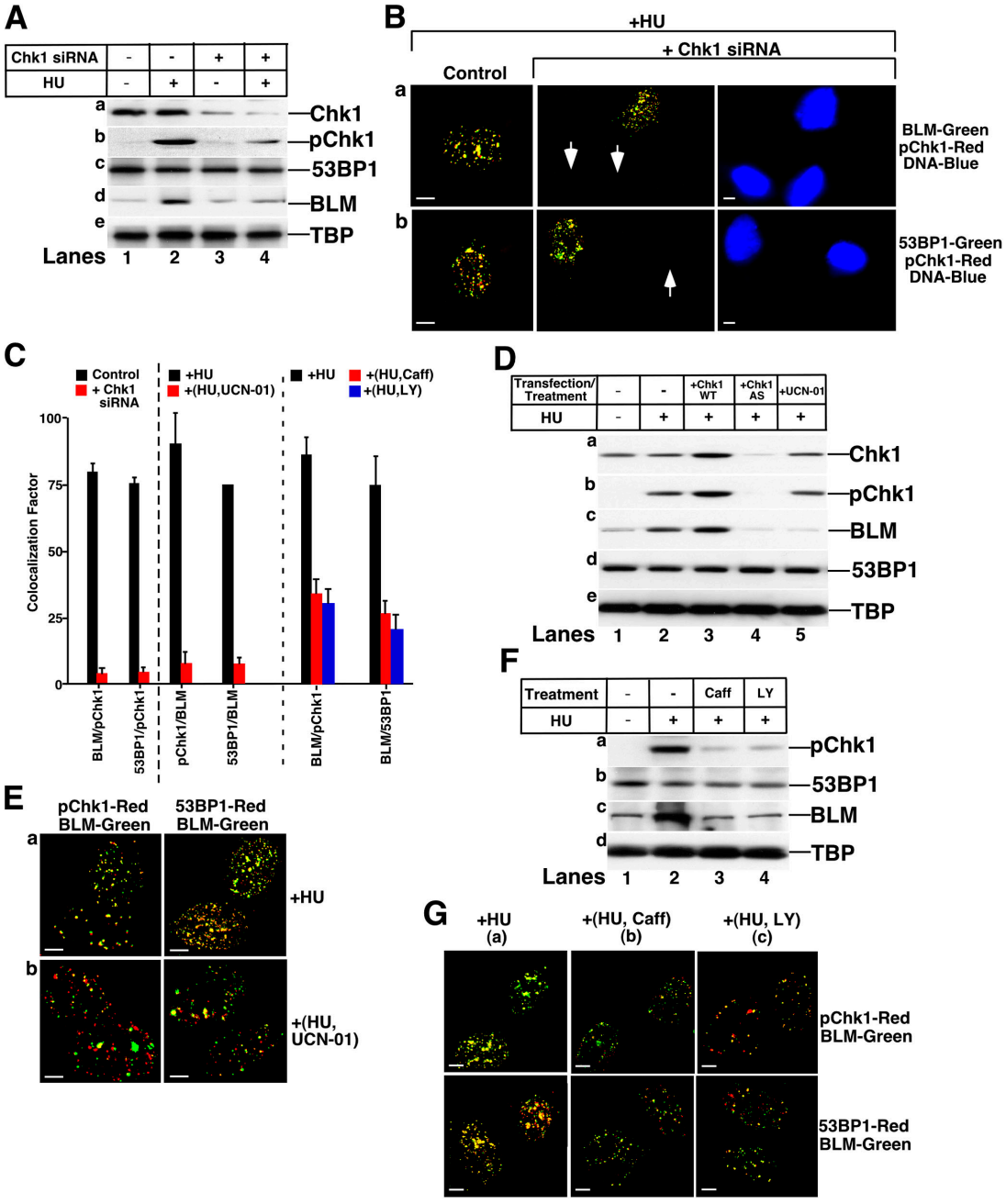

Figure 5. **Accumulation of 53BP1 and BLM depends on the presence of Chk1 and ATR.** (A) The accumulation of proteins in control and Chk1 siRNA-treated NHFs. Control (lanes 1 and 2) or Chk1 siRNA-transfected (lanes 3 and 4) NHFs were contact inhibited, split at low dilution, and grown either in the absence (lanes 1 and 3) or presence (lanes 2 and 4) of HU for 6 h. Western blots were performed with anti-Chk1 (a), anti-pChk1 (b), anti-53BP1 (polyclonal; c), anti-BLM (C-18) (d), and anti-TBP antibodies (e). (B) The lack of Chk1 prevents the accumulation of pChk1, BLM, and p53. NHFs transfection and treatment was done as in A. Immunofluorescence was performed with antibodies against BLM (C-18)/pChk1/DNA (DAPI) (a) and 53BP1 (monoclonal)/pChk1/DNA (DAPI) (b). Fields were chosen that contained a cell in which Chk1 expression was not suppressed as an internal control for the cells lacking expression of Chk1. Arrows indicate position of cells that lack the expression of Chk1. Bars, 5 μm. (C) Quantitations of Fig. 5 (B, E, and G). The histograms represent mean ± SD. (D) The accumulation of proteins in NHFs due to treatment with UCN-01 and the transfection of Chk1 wild-type (WT) or antisense (AS). NHFs, transfected with Chk1 WT (lane 3) or AS (lane 4) were contact inhibited, split at low dilution, and either left untreated (lane 1) or treated with HU (lanes 2–4). Untransfected HU-treated cells were coincubated with UCN-01 (lane 5). Western blots were performed with anti-Chk1 (a), anti-pChk1 (b), anti-BLM (C-18) (c), anti-53BP1 (polyclonal; d), and anti-TBP antibodies (e). (E) UCN-01 inhibits focal colocalization of BLM/53BP1 with pChk1. NHFs were prepared as in D and treated with HU (a) or HU and UCN-01 (b) for 6 h. Immunofluorescence was performed with antibodies against pChk1/BLM (C-18) or 53BP1 (monoclonal)/BLM (ab476). (F) The accumulation of proteins in NHFs after treatment with caffeine and LY294002. NHFs were contact inhibited, split at low dilution, and left either untreated (lane 1) or treated (lanes 2–4) with HU. Coincubation was performed with either caffeine (lane 3) or LY294002 (lane 4). Western blots were performed with anti-pChk1 (a), anti-53BP1 (polyclonal; b), anti-BLM (C-18) (c), and anti-TBP (d) antibodies. Bars, 5 μm. (G) Caffeine and LY294002 inhibit focal colocalization of 53BP1 and BLM. NHFs were prepared as in F and were treated with HU (a); HU and caffeine (b); and HU and LY294002 (c) for 6 h. Immunofluorescence was performed with antibodies against pChk1/BLM (C-18) or 53BP1 (monoclonal)/BLM (ab476). Bars, 5 μm.

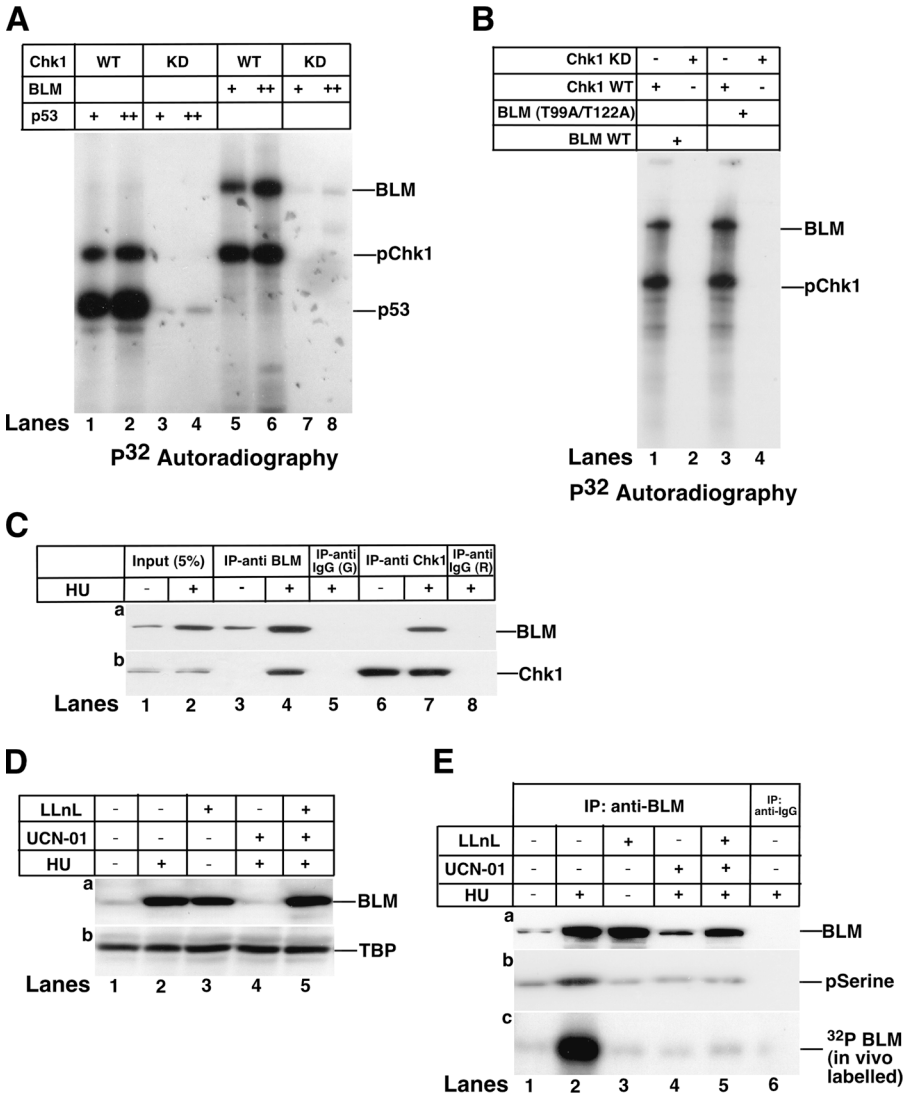

Figure 6. **Chk1-mediated phosphorylation of BLM.** (A) Chk1 phosphorylates p53 and BLM. Recombinant Chk1 (WT or KD) was incubated with full-length p53 or BLM protein in the presence of γ-^{32}P ATP. The proteins were resolved by SDS-PAGE and detected by autoradiography. (B) Chk1 phosphorylates BLM T99A/T122A mutant. Phosphorylation reactions were performed as in A except immunoprecipitated WT BLM or T99A/T122A mutant was used. (C) Chk1 and BLM interact in vivo. NHFs were contact inhibited, split at low dilution, and treated with HU for 6 h. Lysates (2 mg) were immunoprecipitated with antibodies against BLM (ab476) (lanes 3 and 4), Chk1 (lanes 6 and 7), or the corresponding goat IgGs (lane 5, goat; lane 8, rabbit). Input (lanes 1 and 2) indicates 5% of the lysate was used for immunoprecipitation. The blots were probed with BLM (ab476) (a) and Chk1 (b) antibodies. Lanes 1, 3, 6, minus HU; lanes 2, 4, 5, 7, and 8, plus HU. (D) Inhibition of Chk1-mediated phosphorylation destabilizes BLM. NHFs were either left untreated (lane 1) or treated with HU (lane 2), LLnL (lane 3), HU+UCN-01 (lane 4), and HU+UCN-01+LLnL (lane 5). Western blots were performed with anti-BLM (C-18) (a) and anti-TBP (b) antibodies. (E) Chk1-mediated phosphorylation of BLM on serine residues in vivo. NHFs were treated as in D (for a and b) or grown in the presence of phosphate-free DME containing 2 mCi of ^{32}P-labeled inorganic phosphate per ml (for c). Lysates (2 mg) were immunoprecipitated with antibodies against BLM (ab476) (lanes 1–5) or the corresponding IgG (lane 6). The efficiency of immunoprecipitation was verified with (a) BLM (ab476) antibody. Phosphorylation on BLM was detected with phosphoserine antibody (b) or by autoradiography (c).

detected in Chk1 immunoprecipitates (Fig. 6 C). The interaction between Chk1 and BLM occurred only in +HU condition, indicating that Chk1–BLM interaction was a consequence of replicational stress.

To elucidate if BLM stabilization was mediated in vivo by Chk1-mediated phosphorylation during replicational stress, we treated NHFs with HU in the presence or absence of UCN-01 and LLnL (proteosome inhibitor), either singly or in combination. Treatment with LLnL stabilizes BLM to a similar extent as HU. Significantly, UCN-01–mediated decrease in the level of BLM during HU treatment was abrogated in concurrent presence of LLnL (Fig. 6 D). These results suggest that Chk1-mediated phosphorylation of BLM leads to its subsequent stabilization.

Finally, to determine if Chk1-mediated BLM phosphorylation does indeed occur in vivo, we undertook two parallel approaches. First, we immunoprecipitated BLM from cell extracts when NHF was grown in the absence or presence of HU, UCN-01, or LLnL. Correlating with the relative expression levels (Fig. 6 D, a), proportionate amounts of BLM were immunoprecipitated (Fig. 6 E, a). Using an antibody that specifically recognizes phosphoserine residues, we found that immunoprecipitated BLM was hyperphosphorylated on serine residues during replicational stress, i.e., +HU condition. Though BLM was stabilized by LLnL, it was not serine phosphorylated above the background level (Fig. 6 E, b). In a parallel experiment, ^{32}P-radiolabeled endogenous BLM was immunoprecipitated from in vivo labeled cells treated as in Fig. 6 D but grown in the presence of inorganic phosphate. The relative ratio of ^{32}P-labeled immunoprecipitated BLM under different conditions/treatments was similar to those under nonradioactive growth conditions (unpublished data). Hyperphosphorylation of stabilized BLM was detected during HU-mediated replicational stress but not when the helicase was restabilized by LLnL (Fig. 6 E).

Discussion

BLM is phosphorylated by both ATM and ATR sensor kinases (Beamish et al., 2002; Davies et al., 2004). However,

very little is known about how the DNA damage signal is propagated to BLM by the signal transducer proteins from these upstream sensor kinases. Investigating genetically defined and untransformed isogenic human and murine cell lines, we show BLM to be an important responder protein at the core of the replicational stress pathway, possibly involved in relaying the signal due to replicational stress to different effector pathways involved in DNA repair. BLM foci accumulated at the sites of stalled DNA replication forks and DNA strand breaks within 30 min of HU treatment along with the known DNA damage sensor proteins, γ-H2AX and 53BP1, indicating that it was an intermediate responder to certain types of DNA damage (Fig. 1). BLM facilitated the physical interaction of 53BP1 with p53, possibly because of its (BLM's) enhanced accumulation during S-phase (Fig. 2, A–D). However, 53BP1 was functionally upstream of BLM and was required for the focal accumulation of the latter to the sites of stalled replication forks (Figs. 2 F and 3 C and Fig. S2 A). Hence, a regulatory loop exits between BLM and 53BP1 that modulates each other's function. However, from these immunoprecipitation and immunofluorescence experiments we cannot completely rule out the possibility that 53BP1, BLM, and p53 can also be present in a large multiprotein complex.

When exposed to IR, H2AX becomes extensively phosphorylated within 1–3 min of DNA damage and colocalize with proteins involved in both HR and nonhomologous end joining (NHEJ; Paull et al., 2000). As also reported recently (Davalos and Campisi, 2003), BLM foci colocalized appreciably with γ-H2AX, and the extent of colocalization increased with time, reflecting an increase in accumulation of DNA damage (Fig. 1). However, BLM/53BP1 foci had an appreciable degree of colocalization, even in the absence of H2AX (Fig. 4). These results with replicational stress were in contrast to the results with IR regarding γ-H2AX accumulation, where γ-H2AX is crucial for the accumulation of DNA repair complexes on damaged DNA (Bassing et al., 2002; Celeste et al., 2002). In combination with existing literature, our results indicate that (a) the damage induced by replicational stress on the DNA is different from the DSBs induced by IR (or an IR mimicker like NCS), and (b) functional redundancies exists in cells that distinguish the DNA damage sensor proteins and their relative rates of accumulation at the stalled DNA replication forks and DNA strand breaks. Interestingly, H2AX is not required for Chk1 phosphorylation (Ward et al., 2004), validating our hypothesis of a distinct cellular response due to stalled replicational forks. It is possible that BLM plays a role in the phosphorylation of H2AX during DNA damage by acting as an adaptor protein between the kinases and H2AX.

53BP1 foci, but not its protein level, were dependent on the presence of Chk1 (Fig. 5, A, B, and D). Hence, we postulate that Chk1 and/or its activated form served as a scaffolding protein, at which 53BP1 foci could accumulate during replicational stress. 53BP1 is phosphorylated in response to IR in an ATM-dependent pathway (Anderson et al., 2001; Rappold et al., 2001; Fernandez-Capetillo et al., 2002). However, phosphorylation of 53BP1 is not required for its foci formation after IR exposure (Ward et al., 2003a). Hence, apart from acting as a scaffolding protein, Chk1-dependent phosphorylation of 53BP1 can occur during replicational stress, and such a posttranslational modification may be essential for its accurate focal colocalization at stalled replicational forks (Fig. 5 E). These results do not exclude the possibility that 53BP1 can also act upstream of ATR, as it indeed does in the case of ATM (Mochan et al., 2003).

The extensive focal colocalization of pChk1, 53BP1, and BLM in the presence of HU in NHF and WT ATR-expressing U2OS cells, and the lack of such colocalization due to the concomitant presence of PI-3 kinase inhibitors (in NHFs) or in ATR-kd U2OS cells (Fig. 5 G and Fig. S3 D), indicated that the cell cycle checkpoint pathway, triggered by replicational stress, was regulated primarily by ATR via phosphorylation of Chk1 and consequent focal accumulation of 53BP1/BLM. The accumulation of BLM/53BP1 foci was abrogated because of the depletion of Chk1, suggesting that Chk1 could be functionally upstream of both BLM and 53BP1 (Fig. 5 B and Fig. S3 A). BLM protein levels, its focal accumulation and colocalization with pChk1, and 53BP1 were all diminished when the kinase function of Chk1 was inhibited by UCN-01 (Fig. 5, D and E). Apart from Chk1, UCN-01 also inhibits the kinase activities of Chk2 (at a higher concentration) and cTAK1. Chk2 is implicated in an ATM-mediated checkpoint pathway (primarily for DSBs), whereas cTAK1 is required for G2 cell cycle arrest (Busby et al., 2000; Abraham, 2001). Overall, these results (Fig. 5) are consistent with the hypothesis that upon activation of an ATR-mediated checkpoint, BLM is a target of phosphorylation and stabilization mediated by Chk1.

To investigate the possibility that Chk1-mediated phosphorylation of BLM, both in vitro and in vivo experiments were performed. In vitro, WT Chk1 (and not the KD mutant) phosphorylated BLM (Fig. 6 A). In vivo, endogenous Chk1 and BLM colocalized (Fig. 5, B, E, and G) and coimmunoprecipitated (Fig. 6 C) only in the presence of replicational stress. Chk1 mediated the phosphorylation of BLM in vivo on serine residues in HU-treated cells (Fig. 6 E). Lack of BLM phosphorylation (due to UCN-01 treatment) led to proteosome-mediated BLM destabilization and possible degradation (Fig. 6 D). These experiments provide evidence that Chk1-mediated phosphorylation of BLM is a consequence of replicational stress and is involved in its subsequent stabilization. The phosphorylated, and hence, stabilized BLM possibly interacts with 53BP1, enabling BLM accumulation at HU-induced foci and, possibly, the transmission of the DNA damage signal to downstream effector functions. The phosphorylation-mediated stabilization of BLM is in contrast to the role of Chk1 in the regulation of cdc25A levels. Chk1-mediated phosphorylation of cdc25A is coupled to its (cdc25's) increased proteolysis during IR (Sorensen et al., 2003). Hence, Chk1 has multiple functions in the regulation of S-phase checkpoint.

Based on studies with DNA damaging drugs, it has been suggested that an increase in the protein level of BLM was a direct reflection of a G2 function for the helicase (Bischof et al., 2001). One interpretation of our work can be that the destabilization of BLM due to lack of functional Chk1 in the presence of replicational stress may lead to alterations within S-phase. Though we did not see any gross change in the cell cycle profile of HU/UCN-01–treated NHFs in

short 6-h treatments, the intra-S-phase perturbations cannot be ruled out.

The NH_2-terminal region of BLM (1–212) is phosphorylated at Thr-99 and Thr-122 by ATR during HU treatment (Davies et al., 2004). However, other sites on BLM, outside the NH_2-terminal region, may still be phosphorylated by ATR. The ATR-mediated phosphorylation of BLM was not associated with controlling the accumulation of BLM at the stalled DNA replication forks, its subsequent colocalization with proteins involved in the DNA damage response, or in modulating the SCE function of BLM (Davies et al., 2004). Though Chk1 phosphorylates solely on serine residues of its known in vivo substrates (Bartek and Lukas, 2003), it is possible that both Chk1 and ATR could compete for the same site(s) on BLM. Alternatively, because Chk1 phosphorylated the BLM mutants (T99A, T122A, and T99A/T122A) to a similar extent as WT BLM in vitro (Fig. S4 B and Fig. 6 B), Chk1 and ATR may have distinctive patterns of phosphorylation on BLM, leading to divergent functions. Although ATR-mediated threonine phosphorylation of BLM is involved in the recovery of cells from S-phase (Davies et al., 2004), Chk1-mediated serine phosphorylation is involved in BLM stabilization and its possible interaction with 53BP1 and subsequent signal transduction machinery.

Based on the aforementioned evidence, we propose that BLM acts as a major "molecular node" in response to replicational stress. BLM receives the DNA damage signal from ATR, Chk1, and 53BP1 and, in turn, transmits the signal to different downstream repair processes. BLM attempts to process the stalled forks by reverse branch migration especially in the absence of significant stress. However, as DNA damage accumulates in number and complexity, BLM transmits the signal to pro-recombinogenic RAD51 protein, which resolves the stalled DNA replication forks by HR (Karow et al., 2000; Sengupta et al., 2003). BLM is required for p53 accumulation at stalled DNA replication forks. p53 governs RAD51-dependent gene conversion via direct binding (for review see Bertrand et al., 2004). The suppression of crossing over and the resolution of recombination intermediates due to the functional interaction of BLM and TopoIIIα (Wu and Hickson, 2003) may be a necessary step for the suppression of tumorigenesis.

BLM may be involved in transmitting the signal to both HR and NHEJ, two of the major DNA repair pathways. BLM is required for correct nuclear localization of RAD50/MRE11/NBS1 complexes after replication fork arrest (Franchitto and Pichierri, 2002; Davalos and Campisi, 2003). BLM is also involved in the alignment of microhomology elements during NHEJ (Langland et al., 2002). Functional cross-talk exists in cells between BLM and members of the mismatch repair pathway. ATR, BLM, and MSH6 are part of the BASC complex (Wang et al., 2000). Recently, we have reported that MSH2/6 colocalize, physically interact, and stimulate the helicase function of BLM (Yang et al., 2004).

In conclusion, we provide compelling evidence that both 53BP1 and BLM are responders during replicational stress. Whereas BLM facilitates the physical interaction between p53 and 53BP1, 53BP1 is responsible for the accumulation of BLM foci at stalled replication forks. The accumulation of BLM/53BP1 foci and the physical interaction between them is not dependent on γ-H2AX. ATR and Chk1 are functionally upstream of BLM. Chk1 regulates the accumulation of 53BP1/BLM foci and BLM stabilization via phosphorylation. This work provides direct evidence of BLM as a protein involved in signal transduction during replicational stress.

Materials and methods

Antibodies

The antibodies used were as follows: Anti-p53: monoclonals DO-1 (Santa Cruz Biotechnology, Inc.); rabbit polyclonal CM1 (Signet). Anti-BLM: goat polyclonal C-18 (Santa Cruz Biotechnology, Inc.); rabbit polyclonal ab476 (Novus). Anti-BrdU: monoclonal (Amersham Biosciences). Anti-53BP1: monoclonal (Schultz et al., 2000); rabbit polyclonal (Anderson et al., 2001). Anti-γ-H2AX: rabbit polyclonal PC-100 (Trevigen). Anti-TBP: monoclonal 58C9 (Santa Cruz Biotechnology, Inc.). Anti-Chk1: rabbit polyclonal #2345 (Cell Signaling). Anti-phospho-Chk1 (Ser317): rabbit polyclonal #2344 (Cell Signaling). Antiphosphoserine: monoclonal (Sigma-Aldrich). Anti-Nucleolin (C23): monoclonal MS-3 (Santa Cruz Biotechnology, Inc.). Secondary antibodies were purchased from Jackson ImmunoResearch Laboratories and Southern Biotechnology Associates, Inc.

Cells, culture conditions, and treatments

HTERT-immortalized NHF strain GM07532 (NHF), GM07532 E6 (NHF E6), hTERT-immortalized Bloom syndrome, BS, fibroblasts and chromosome-15-corrected BS fibroblasts, BS A-15 (GM03509 A-15; Sengupta et al., 2003); WT and KO primary 53BP1 MEFs (Ward et al., 2003b); and WT and KO H2AX MEFs (Celeste et al., 2002) were maintained as published. BS and BS A-15 were provided by J. Shay (University of Texas, Southwestern Medical Center at Dallas, Dallas, TX).

HU (Sigma-Aldrich; 1 mM, indicated time intervals) and BrdU (Sigma-Aldrich; 150 μM for 10 min) treatments were done as described previously (Linke et al., 2003; Sengupta et al., 2003). In short, cells were synchronized in G0 by growth to confluence, plated at low density for 24 h so that most of the cells are in G1/S boundary. Cells were either left untreated or treated with HU for indicated time intervals. Incubation of NHFs with 100 nM UCN-01 (NCI/NIH), 4 mM of caffeine (Sigma-Aldrich), and 50 μM LY294002 (Cell Signaling) was performed 1 h before, and for the duration of HU treatment. 50 μM LLnL (also known as ALLN or MG-101; Sigma-Aldrich) was used during the HU treatment.

siRNA and AS transfection

Based on published sequences, siRNA for 53BP1 (DiTullio et al., 2002) and Chk1 (Zhao et al., 2002) were synthesized by Dharmacon Research. Scrambled duplex RNA, luciferase siRNA, and mock transfection were used as controls. siRNAs were transfected by transfection reagent (Mirus Corporation) according to the manufacturer's protocol. Transfections with each siRNA were done twice for every experiment. Posttransfected cells were synchronized in G0 by growth to confluence, released at low dilutions for 24 h, and subsequently treated with HU. Experiments were repeated three times and the cells were analyzed 48 h after transfection. Transfections with Chk1 sense (provided by C. Prives, Columbia University, New York, NY) and AS (provided by S.-Y. Shieh, Academia Sinica, Taipei, Taiwan) constructs were carried out using Lipofectamine 2000 (Invitrogen), according to the manufacturer's protocol.

Western blots and immunoprecipitations

Cells were lysed in modified RIPA buffer (1 mM Tris HCl, pH 7.4, 150 mM NaCl, 1% sodium deoxycholate, 0.1% SDS, 1mM PMSF, and protease inhibitors) for Western blot analysis or immunoprecipitation buffer (50 mM Tris HCl, pH 8.0, 20% glycerol, 1 mM DTT, 0.1% NP-40, 500 mM KCl, and protease inhibitors) for immunoprecipitations, as described previously (Sengupta et al., 2003). Greater than 90% of the BLM was released from the chromatin using the modified RIPA buffer. Western blot analysis and immunoprecipitations were performed by standard protocols. The experiments were repeated twice and representative blots are shown.

Microscopy

The cells were grown on coverslips in 6-well plates. Immunofluorescence was performed as described previously (Sengupta et al., 2003). In short, the cells were subjected to preextraction, which removed the soluble proteins present in the nucleoplasm. The nucleus with proteins bound to the insolu-

ble DNA matrix were fixed and stained. The sites of nascent DNA replication were detected by anti-BrdU antibodies after Dnase treatment (Kennedy et al., 2000) and visualized in a fluorescent microscope (model Axioskop; Carl Zeiss MicroImaging, Inc.) equipped with a high performance CCD imaging system (IP Lab Spectrum). Alternatively, confocal fluorescent images were collected with a confocal scan head (model MRC 1024; Bio-Rad Laboratories) mounted on a microscope (model Optiphot; Nikon) with a 60× objective. Images were analyzed by software (Bio-Rad Laboratories). At least 100 cells were analyzed for each colocalization experiment. The experiments were repeated twice. Colocalization factor is defined as [(Fraction of cells having colocalization) × (Fraction of foci colocalized per cell)] × 100. For example, if 90% of the cells (fraction = 0.9) show colocalization, and on an average 70% of the foci colocalized per cell (fraction = 0.7), then the colocalization factor is (0.9 × 0.7) × 100 = 63.

Labeling and kinase assays

Chk1 kinase assays were performed with 300 ng of the kinase (WT or KD) and purified His-tagged BLM (150 and 300 ng) or p53 (75 and 150 ng) according to published protocols (Shieh et al., 2000). Chk1 WT and KD recombinant proteins were provided by C. Prives. p53 protein was purchased from Protein One. Purification of Chk1 and BLM have been reported previously (Shieh et al., 2000; Yang et al., 2004). Flag-tagged pcDNA BLM (WT and mutant; T99A/T122A) have been described previously (Davies et al., 2004) and were provided by I. Hickson (Cancer Research UK Laboratories, Oxford, UK). NHFs were transfected with the BLM constructs, and the helicase was immunoprecipitated and used for in vitro phosphorylation reactions. For in vivo ^{32}P labeling, NHFs were grown for 6 h in phosphate-free DME containing 2 mCi of ^{32}P-labeled inorganic phosphate per milliliter in the presence of the treatments, as described.

Online supplemental material

Fig. S1 shows colocalization of 53BP1 with MRE11 and RAD51 at the sites of stalled DNA replicational forks. Fig. S2 shows specificity of 53BP1 siRNA and the cell cycle profiles after 53BP1 siRNA transfection. Fig. S3 shows specificity of Chk1 siRNA and decreased colocalization of pChk1, 53BP1, and BLM in the absence of functional ATR. Fig. S4 shows Chk1-mediated in vitro phosphorylation on the NH_2-terminal (1–212) BLM fragment. Online supplemental material (Figs. S1–S4) is available at http://www.jcb.org/cgi/content/full/jcb.200405128/DC1.

We thank Carol Prives, Sheau-Yann Shieh, Ian Hickson, and Jerry Shay for recombinant proteins, plasmids, and cells. We thank Susan Garfield for assistance in confocal microscopy. We also thank Dorothea Dudek for editorial assistance and Karen MacPherson for bibliographic assistance.

Submitted: 21 May 2004
Accepted: 8 July 2004

References

Abraham, R.T. 2001. Cell cycle checkpoint signaling through the ATM and ATR kinases. *Genes Dev.* 15:2177–2196.

Anderson, L., C. Henderson, and Y. Adachi. 2001. Phosphorylation and rapid relocalization of 53BP1 to nuclear foci upon DNA damage. *Mol. Cell. Biol.* 21:1719–1729.

Bartek, J., and J. Lukas. 2003. Chk1 and Chk2 kinases in checkpoint control and cancer. *Cancer Cell.* 3:421–429.

Bassing, C.H., K.F. Chua, J. Sekiguchi, H. Suh, S.R. Whitlow, J.C. Fleming, B.C. Monroe, D.N. Ciccone, C. Yan, K. Vlasakova, et al. 2002. Increased ionizing radiation sensitivity and genomic instability in the absence of histone H2AX. *Proc. Natl. Acad. Sci. USA.* 99:8173–8178.

Beamish, H., P. Kedar, H. Kaneko, P. Chen, T. Fukao, C. Peng, S. Beresten, N. Gueven, D. Purdie, S. Lees-Miller, et al. 2002. Functional link between BLM defective in Bloom's syndrome and the ataxia-telangiectasia-mutated protein, ATM. *J. Biol. Chem.* 277:30515–30523.

Bertrand, P., Y. Saintigny, and B.S. Lopez. 2004. p53's double life: transactivation-independent repression of homologous recombination. *Trends Genet.* 20:235–243.

Bischof, O., S.H. Kim, J. Irving, S. Beresten, N.A. Ellis, and J. Campisi. 2001. Regulation and localization of the Bloom syndrome protein in response to DNA damage. *J. Cell Biol.* 153:367–380.

Busby, E.C., D.F. Leistritz, R.T. Abraham, L.M. Karnitz, and J.N. Sarkaria. 2000. The radiosensitizing agent 7-hydroxystaurosporine (UCN-01) inhibits the DNA damage checkpoint kinase hChk1. *Cancer Res.* 60:2108–2112.

Celeste, A., S. Petersen, P.J. Romanienko, O. Fernandez-Capetillo, H.T. Chen, O.A. Sedelnikova, B. Reina-San-Martin, V. Coppola, E. Meffre, M.J. Difilippantonio, et al. 2002. Genomic instability in mice lacking histone H2AX. *Science.* 296:922–927.

Davalos, A.R., and J. Campisi. 2003. Bloom syndrome cells undergo p53-dependent apoptosis and delayed assembly of BRCA1 and NBS1 repair complexes at stalled replication forks. *J. Cell Biol.* 162:1197–1209.

Davies, S.L., P.S. North, A. Dart, N.D. Lakin, and I.D. Hickson. 2004. Phosphorylation of the Bloom's syndrome helicase and its role in recovery from S-phase arrest. *Mol. Cell. Biol.* 24:1279–1291.

DiTullio, R.A., Jr., T.A. Mochan, M. Venere, J. Bartkova, M. Sehested, J. Bartek, and T.D. Halazonetis. 2002. 53BP1 functions in an ATM-dependent checkpoint pathway that is constitutively activated in human cancer. *Nat. Cell Biol.* 4:998–1002.

Fernandez-Capetillo, O., H.T. Chen, A. Celeste, I. Ward, P.J. Romanienko, J.C. Morales, K. Naka, Z. Xia, R.D. Camerini-Otero, N. Motoyama, et al. 2002. DNA damage-induced G2-M checkpoint activation by histone H2AX and 53BP1. *Nat. Cell Biol.* 4:993–997.

Franchitto, A., and P. Pichierri. 2002. Bloom's syndrome protein is required for correct relocalization of RAD50/MRE11/NBS1 complex after replication fork arrest. *J. Cell Biol.* 157:19–30.

Hickson, I.D. 2003. RecQ helicases: caretakers of the genome. *Nat. Rev. Cancer.* 3:169–178.

Iwabuchi, K., P.L. Bartel, B. Li, R. Marraccino, and S. Fields. 1994. Two cellular proteins that bind to wild-type but not mutant p53. *Proc. Natl. Acad. Sci. USA.* 91:6098–6102.

Karow, J.K., A. Constantinou, J.L. Li, S.C. West, and I.D. Hickson. 2000. The Bloom's syndrome gene product promotes branch migration of holliday junctions. *Proc. Natl. Acad. Sci. USA.* 97:6504–6508.

Kennedy, B.K., D.A. Barbie, M. Classon, N. Dyson, and E. Harlow. 2000. Nuclear organization of DNA replication in primary mammalian cells. *Genes Dev.* 14:2855–2868.

Langland, G., J. Elliott, Y. Li, J. Creaney, K. Dixon, and J. Groden. 2002. The BLM helicase is necessary for normal DNA double-strand break repair. *Cancer Res.* 62:2766–2770.

Linke, S.P., S. Sengupta, N. Khabie, B.A. Jeffries, S. Buchhop, S. Miska, W. Henning, R. Pedeux, X.W. Wang, L.J. Hofseth, et al. 2003. p53 interacts with hRAD51 and hRAD54, and directly modulates homologous recombination. *Cancer Res.* 63:2596–2605.

Mochan, T.A., M. Venere, R.A. DiTullio Jr., and T.D. Halazonetis. 2003. 53BP1 and NFBD1/MDC1-Nbs1 function in parallel interacting pathways activating ataxia-telangiectasia mutated (ATM) in response to DNA damage. *Cancer Res.* 63:8586–8591.

Nghiem, P., P.K. Park, Y.S. Kim, B.N. Desai, and S.L. Schreiber. 2002. ATR is not required for p53 activation but synergizes with p53 in the replication checkpoint. *J. Biol. Chem.* 277:4428–4434.

Paull, T.T., E.P. Rogakou, V. Yamazaki, C.U. Kirchgessner, M. Gellert, and W.M. Bonner. 2000. A critical role for histone H2AX in recruitment of repair factors to nuclear foci after DNA damage. *Curr. Biol.* 10:886–895.

Povirk, L.F., C.W. Houlgrave, and Y.H. Han. 1988. Neocarzinostatin-induced DNA base release accompanied by staggered oxidative cleavage of the complementary strand. *J. Biol. Chem.* 263:19263–19266.

Rappold, I., K. Iwabuchi, T. Date, and J. Chen. 2001. Tumor suppressor p53 binding protein 1 (53BP1) is involved in DNA damage–signaling pathways. *J. Cell Biol.* 153:613–620.

Rogakou, E.P., C. Boon, C. Redon, and W.M. Bonner. 1999. Megabase chromatin domains involved in DNA double-strand breaks in vivo. *J. Cell Biol.* 146: 905–916.

Sarkaria, J.N. 2003. Identifying inhibitors of ATM and ATR kinase activities. *Methods Mol. Med.* 85:49–56.

Schultz, L.B., N.H. Chehab, A. Malikzay, and T.D. Halazonetis. 2000. p53 binding protein 1 (53BP1) is an early participant in the cellular response to DNA double-strand breaks. *J. Cell Biol.* 151:1381–1390.

Sengupta, S., S.P. Linke, R. Pedeux, Q. Yang, J. Farnsworth, S.H. Garfield, K. Valerie, J.W. Shay, N.A. Ellis, B. Wasylyk, and C.C. Harris. 2003. BLM helicase-dependent transport of p53 to sites of stalled DNA replication forks modulates homologous recombination. *EMBO J.* 22:1210–1222.

Shieh, S.Y., J. Ahn, K. Tamai, Y. Taya, and C. Prives. 2000. The human homologs of checkpoint kinases Chk1 and Cds1 (Chk2) phosphorylate p53 at multiple DNA damage-inducible sites. *Genes Dev.* 14:289–300.

Sorensen, C.S., R.G. Syljuasen, J. Falck, T. Schroeder, L. Ronnstrand, K.K.

Khanna, B.B. Zhou, J. Bartek, and J. Lukas. 2003. Chk1 regulates the S phase checkpoint by coupling the physiological turnover and ionizing radiation-induced accelerated proteolysis of Cdc25A. *Cancer Cell.* 3:247–258.

Suzuki, T., M. Shiratori, Y. Furuichi, and T. Matsumoto. 2001. Diverged nuclear localization of Werner helicase in human and mouse cells. *Oncogene.* 20:2551–2558.

van Brabant, A.J., R. Stan, and N.A. Ellis. 2000. DNA helicases, genomic instability, and human genetic disease. *Annu. Rev. Genomics Hum. Genet.* 1:409–459.

Wang, B., S. Matsuoka, P.B. Carpenter, and S.J. Elledge. 2002. 53BP1, a mediator of the DNA damage checkpoint. *Science.* 298:1435–1438.

Wang, X.W., A. Tseng, N.A. Ellis, E.A. Spillare, S.P. Linke, A.I. Robles, H. Seker, Q. Yang, P. Hu, S. Beresten, et al. 2001. Functional interaction of p53 and BLM DNA helicase in apoptosis. *J. Biol. Chem.* 276:32948–32955.

Wang, Y., D. Cortez, P. Yazdi, N. Neff, S.J. Elledge, and J. Qin. 2000. BASC, a super complex of BRCA1-associated proteins involved in the recognition and repair of aberrant DNA structures. *Genes Dev.* 14:927–939.

Ward, I.M., K. Minn, K.G. Jorda, and J. Chen. 2003a. Accumulation of checkpoint protein 53BP1 at DNA breaks involves its binding to phosphorylated histone H2AX. *J. Biol. Chem.* 278:19579–19582.

Ward, I.M., K. Minn, J. van Deursen, and J. Chen. 2003b. p53 Binding protein 53BP1 is required for DNA damage responses and tumor suppression in mice. *Mol. Cell. Biol.* 23:2556–2563.

Ward, I.M., K. Minn, and J. Chen. 2004. UV-induced ataxia-telangiectasia-mutated and Rad3-related (ATR) activation requires replication stress. *J. Biol. Chem.* 279:9677–9680.

Wu, L., and I.D. Hickson. 2003. The Bloom's syndrome helicase suppresses crossing over during homologous recombination. *Nature.* 426:870–874.

Wu, L., S.L. Davies, N.C. Levitt, and I.D. Hickson. 2001. Potential role for the BLM helicase in recombinational repair via a conserved interaction with RAD51. *J. Biol. Chem.* 276:19375–19381.

Yang, Q., R. Zhang, X.W. Wang, S.P. Linke, S. Sengupta, I.D. Hickson, G. Pedrazzi, C. Perrera, I. Stagljar, S.J. Littman, et al. 2004. The mismatch DNA repair heterodimer, hMSH2/6, regulates BLM helicase. *Oncogene.* 23:3749–3756.

Zhao, H., J.L. Watkins, and H. Piwnica-Worms. 2002. Disruption of the checkpoint kinase 1/cell division cycle 25A pathway abrogates ionizing radiation-induced S and G2 checkpoints. *Proc. Natl. Acad. Sci. USA.* 99:14795–14800.